

Synthesis and characterization of physicochemical properties of imidazolium-based ionic liquids and their application for simultaneous determination of sulfur compounds



Seyed Mohammad Reza Shoja^a, Majid Abdouss^{a,*}, Ali Akbar Miran Beigi^b

^a Department of Chemistry, Amirkabir University of Technology, P.O. Box 15875-4413, Tehran, Iran

^b Research Institute of Petroleum Industry(RIPI), P.O. Box 14665-1998, Tehran, Iran

ARTICLE INFO

Article history:

Received 13 July 2020

Revised 4 November 2020

Accepted 8 January 2021

Available online 11 January 2021

Keywords:

Imidazolium-based ionic liquids

Physicochemical properties

Temperature-Dependence

Scavengers

ABSTRACT

Three types of imidazolium-based ionic liquids (IMILs) were synthesized and characterized by ¹³C and ¹H NMR, FT-IR, and elemental analysis. Thermal stability and physicochemical properties of prepared IMILs were measured in the temperature range of 283.15 to 363.15 K. The physicochemical results revealed the entirely temperature-dependent properties and quietly decreasing through increasing the temperature. Electrochemical studies of the IMILs were also performed at the surface of screen-printed electrode cells. Consideration of these properties and determining the unique abilities of IMILs will help researchers through modern applications like liquid-liquid extraction, particular tasks of scavenging and removal of hydrogen sulfide and thiols from petroleum matrices.

© 2021 Elsevier B.V. All rights reserved.

1. Introduction

Recently, the major vital and prolific eco-friendly features of green chemistry has been flourished in science and engineering. The main focuses were on decreasing the number of toxic solvents and reagents within an analysis procedure, reducing the consumed energy, produced wastes, and increasing reusability of solvents. Hence, many efforts have been prepared to formulate new green reaction media and solvents in all science [1–4]. A few decades ago, many studies were devoted to evaluating the synthesis and characterization of ionic liquids (ILs), a favored eco-friendly alternative for common solvents [5–8].

ILs, entirely prepared using cations and anions, possess a dissolving point of 373.15 K or below. In this manner, they would highlight the advantages of available replacements for dangerous and unstable materials due to their unique physicochemical properties [9–13]. The main interest was attracted toward ILs as the “designer” solvent [14–17] in many fields such as the oil industry [18–20], biotechnology, material science [21–23], electrochemistry, solvent effect, separation [24–30], fuel cells, nanotechnology [31–35], catalysts and as a reaction medium in the irreversible reaction of H₂S to form a thermally stable, oil-soluble alkyl sulfide [36,37] thanks to their high thermal and chemical stabilities, low

volatility and melting point, non-flammability, high ionic conductivity, the broad range of electrochemical properties, and tunable polarity [13,38–40].

To further evaluate the intrinsic properties of ILs and to discover their specific applications as pollutant scavenger and electrolyte, it is required to understand their thermophysical and electrochemical properties. It is possible to project the industrial processes and new ILs-based products when the physicochemical properties of these ILs such as viscosity, density, surface tension, refractive index, and thermal decomposition are pointed out [41].

Currently, imidazolium and dialkyl imidazolium-based ILs were the most stable and commonly used ILs. Simultaneously, the highest studied ILs types and numerous attempts have been made in preparation for pure and halogen-free imidazolium-based ILs [42–45]. The physicochemical properties of imidazolium-based ILs can be adjusted by slight structural modifications of the corresponding cation, anion, and alkyl chain length [36,46,47]. Likewise, the structure and type of anions and cations would help regulate the hydrophilicity and hydrophobicity of ILs. Shorter and longer alkyl side chains could result in higher hydrophilicity and hydrophobicity, respectively [48].

In this research work, we selected three hydrophilic ionic liquids with a limited database regarding their physicochemical properties and the simultaneous determination of sulfur compounds. Therefore, to investigate the effect of anions, cations, cation-linked functional groups, and impact of molecular symmetry, three different imidazolium-based ionic liquids,

* Corresponding author.

E-mail address: phdabdouss44@aut.ac.ir (M. Abdouss).

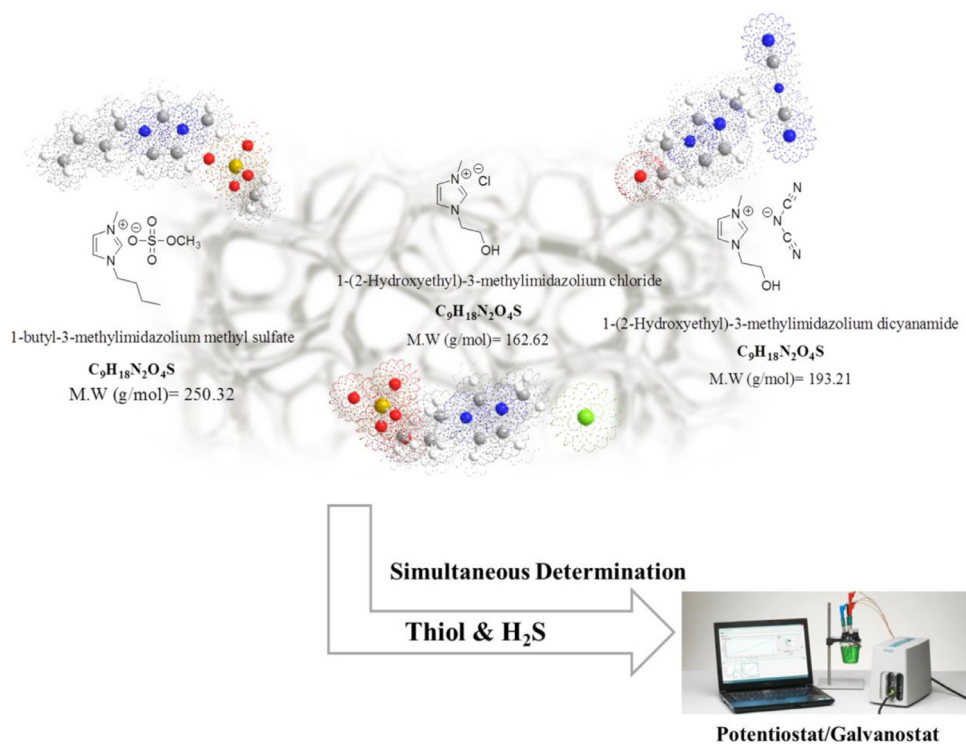


Fig. 1. Chemical structures of the prepared ionic liquids.

1-butyl-3-methylimidazolium methyl sulfate [BMIM][MeSO₄], 1-(2-Hydroxyethyl)-3-methylimidazolium chloride [HEMIM][Cl] and 1-(2-Hydroxyethyl)-3-methylimidazolium dicyanamide [HEMIM][DCA] were pointed to synthesize and evaluate the physicochemical properties in the wide range of temperature for the first time. The ionic liquids were also characterized using ¹³C and ¹H NMR, FT-IR, and CHNOS elemental analysis. Given that the available standard methods, like UOP-163 [49], suffer from interfering constituents in the sample matrix and are very time-consuming, using large sample size and toxic solvents, the other purpose of this research was a development of methodology by using a new ILs for determination of certain organic pollutants such as H₂S and R-SH, so we also used synthesized ILs for the first time as an ideal medium for electroanalytical determination of these species in petroleum matrices. The chemical structures of the prepared ILs were illustrated in Fig. 1.

2. Experimental

2.1. Materials

1-methylimidazole ($\geq 99\%$), 1-butyl imidazole ($\geq 98\%$), and 2-chloroethanol ($\geq 99\%$) were pursued from Aldrich and were distilled before use. All other starting materials and solvents were used as received without any further consideration. These materials included dimethyl sulfate ($\geq 99\%$), methylene chloride ($\geq 99\%$), sodium dicyanamide ($\geq 96\%$), diethyl ether ($\geq 99\%$), toluene ($\geq 99.8\%$) and acetone ($\geq 99\%$). All of them purchased from Aldrich too. Water was freshly deionized and distilled before use.

2.2. Apparatus and procedure

The structures of synthesized ILs were identified by ¹³C and ¹H NMR (Bruker Avance 500 MHz spectrometers, Germany), FT-IR (Bruker Vertex 70 Spectrometer, Germany), and CHNOS elemental analysis (Elementar Vario max, Germany). The density

and dynamic viscosity of the ILs were measured with an automated Anton Paar SVM-3000 (Austria) digital double-tube viscometer. The precision in experimental measurements has been established to be better than $\pm 2 \times 10^{-4} \text{ g}\cdot\text{cm}^{-3}$ for the density and $\pm 1 \times 10^{-4} \text{ mPa}\cdot\text{s}$ for the dynamic viscosity. The instrument was calibrated and certified by the supplier company. The calibration was monitored in the interval mode with pure liquids (supplied by Cannon Co.) with known density, dynamic and kinematic viscosity at different temperatures. The surface tension of the ILs was recorded with a KRUSS-K9 tensiometer (Germany) by the ring method. The measurement cell was thermostated in a temperature controller with temperature stability of $\pm 273.17 \text{ K}$, regulated in the RC6 LAUDA thermostat. The equipment has a digital control unit for precise measurements with an uncertainty better than $\pm 0.1 \text{ mN}\cdot\text{m}^{-1}$. Refractive indices were determined by using a refractometer Model J357 supplied by Rudolph Company (USA). The apparatus was calibrated with isopropyl alcohol and water at different temperatures from 283 to 363 K. Conductivity was dignified with WTW-LF96 (H. Jürgens GmbH & Co. Germany) conductivity meter. The instrument was calibrated and patterned with a standard conductivity solution (1413 $\mu\text{S}/\text{cm}$ at 298 K). The pH, chloride, and bromide content were measured with the Mettler-DL40GP potentiometer (Switzerland). The instrument was calibrated with pH buffers (4, 9, and 11), sodium chloride, and potassium bromide as a primary standard. MKC-501-N, coulometric Karl Fischer apparatus supplied by KEM (Japan), was used to determine trace amounts of water in ILs. Electrochemical measurements were carried out by screen-printed voltammetry Autolab PGSTAT101, supplied by Metrohm Co. (Switzerland) using a three-electrode cell consisted of a glassy carbon working electrode and Ag plate as the reference electrode. A simultaneous TG/DTA thermal analyzer (Perkin Elmer PYRIS Diamond, USA) was used to study the ionic liquids' thermal stability. Approximately 20 mg of the sample and reference (Pt foil) were placed in alumina pans and heated by a rate of $10 \text{ K}\cdot\text{min}^{-1}$ from 298 to 873 K. In this study, the flow rate of nitrogen as purge gas was $50 \text{ mL}\cdot\text{min}^{-1}$ at 1 bar. TG mass and temperature calibrations were performed before the experiments.

2.3. Synthesis of 1-butyl-3-methylimidazolium methyl sulfate

Dimethyl sulfate (150 mL) was added dropwise to a solution of equal molar amounts of 1-butylimidazole (50 g) in toluene at 277.15 K. The reaction mixture was then stirred for 4 h at room temperature. All experiments were performed under the fume hood with a nitrogen gas stream. The upper organic phase of the resulting mixture was decanted, and the lower ionic liquid phase was washed with diethyl ether several times. After the last washing, the remaining diethyl ether solvent was evaporated under reduced pressure. The prepared IL ([BMIM][MeSO₄]) was dried by heating under a high vacuum for 48 h. [BMIM][MeSO₄] was characterized by ¹³C and ¹H NMR, FT-IR, and CHNOS elemental analysis, to prove the absence of impurities.

[BMIM][MeSO₄]: ¹H NMR (500 MHz, D₂O): δ_H 9.12 (s, 1H), 7.34–7.38 (m, unresolved, 2H), 4.00 (t, J = 7.5 Hz, 2H), 3.75 (s, 3H), 3.43 (s, 3H), 1.63 (p, J = 7.5 Hz, 2H), 1.12 (m, J = 7.6 Hz, 2H), 0.66 (t, J = 7.26 Hz, 3H); ¹³C NMR (CDCl₃, 75.4 MHz) δ_C 13.3 (CH₂CH₃), 19.3 (CH₂CH₃), 32.0 (NCH₂CH₂), 36.3 (NCH₃), 49.7 (NCH₂), 54.3 (OCH₃), 122.2 (CH), 123.8 (CH), 137.3 (CH).

2.4. Synthesis of 1-(2-Hydroxyethyl)-3-methylimidazolium chloride

2-chloroethanol (0.67 mL) was reacted with an excess of 1-methyl imidazole (1.1 g) in a round-bottom flask in acetonitrile for 24 h at 393.15 K. These experiments were performed under the fume hood with a nitrogen gas stream. The crude product was recrystallization, finely crushed, and washed with diethyl ether several times. Then, the remained solvent was evaporated under reduced pressure for 10 h to produce the IL. [HEMIM][Cl] was characterized by ¹³C and ¹H NMR, FT-IR, and CHNOS elemental analysis, to prove the absence of impurities.

[HEMIM][Cl]: ¹H NMR (500 MHz, D₂O): δ_H 8.78 (s, 1H, H-2), 7.54 (s, 1H, H-4 or H-5), 7.49 (s, 1H, H-4 or H-5), 4.34 (t, 2H, J = 4.9 Hz), 3.96 (t, 2H, J = 4.9 Hz), 3.93 (s, 3H); ¹³C NMR (CDCl₃, 75.4 MHz), δ_C 136.25 (CH), 123.70 (CH), 122.59 (CH), 59.96 (–CH₂–OH), 51.72 (N–CH₂–), 36.02 (N–CH₃)

2.5. Synthesis of 1-(2-Hydroxyethyl)-3-methylimidazolium dicyanamide

[HEMIM][Cl] (10 g) was added into NaN(CN)₂ (5.6 g) in acetone (20 mL) and stirred at room temperature for 48 h and then filtered. Mentioned experiments were performed under the fume hood with a nitrogen gas stream. After the solvent was removed by rotary evaporation, the residual liquid was diluted with methylene chloride and filtered again. The solvent was removed using rotary evaporation and the remained sample was dried under vacuum at 343 K for 48 h. The final product ([HEMIM][DCA]) was obtained as a colorless condensed liquid. [HEMIM][DCA] was characterized by ¹³C and ¹H NMR, FT-IR, and CHNOS elemental analysis, to prove the absence of impurities.

[HEMIM][DCA]: ¹H NMR (500 MHz, D₂O): δ_H 9.060 (s, 1H), 7.699 (d, 1H), 7.666 (d, 1H), 5.147 (t, 1H), 4.204 (t, 2H), 3.863 (s, 3H), and 3.718 (m, 2H); ¹³C NMR (CDCl₃, 75.4 MHz), δ_C 137.15 (CH), 123.86 (CH), 123.19 (CH), 60.06 (–CH₂–OH), 51.92 (N–CH₂–), 36.92 (N–CH₃) 119.52 (CN).

3. Result and discussion

3.1. Characterization of synthesized imidazolium-based ILs

FT-IR spectra of the synthesized ionic liquids were illustrated in Fig. 2. The FT-IR vibrations at 1225, 1105, and 566 cm⁻¹ were assigned to the S–O bond of sulfonic acid and SO₃⁻ group (asymmetric stretching, symmetric stretching, and bending modes, respec-

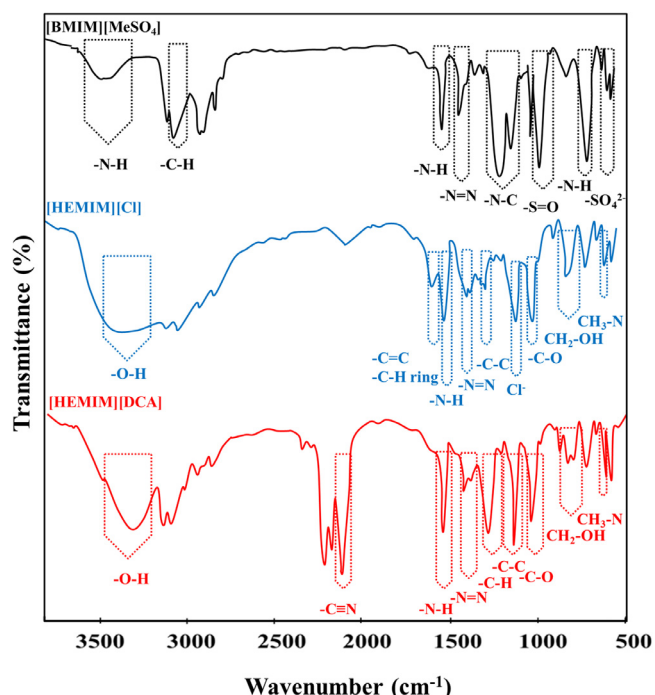


Fig. 2. FT-IR spectra of the prepared ionic liquids.

tively. The N–S stretching vibration was also observed at 880 cm⁻¹. This clear infrared peak stipulated the presence of sulfonic group-pyridine bond in [BMIM][MeSO₄]. The influential bands around 1550 cm⁻¹ from the pyridinium ring were also present in all three ionic liquids. The broad and strong bands in the range of 3000 to 3500 cm⁻¹ can be given to the hydroxyl group (the stretching vibration) due to the presence of water and sulfonic acid (Fig. 2). The details of the FT-IR spectra were depicted in Table 1. Elemental analysis and impurity contents of studied ILs were reported in Fig. 3 and Table 2, respectively. As shown in Fig. 3, the experimental data of C%, N%, O%, H% and S% for all prepared ILs were close to the calculated ones. In Table 2, four test methods of Karl Fischer, Potentiometry, Turbidimetry, Electric furnace, and gravimetry were used to evaluate the impurity contents of prepared ILs. Based on the obtained results, the negligible amount of water content (mass%), chloride (mass%), bromide (ppm), sulfate (ppm), heavy metals (ppm), and ash content (mass%) were detected.

3.2. Physicochemical properties of ILs

The experimental data on the physicochemical properties of studied ILs were itemized in the temperature range of 283.15 to 363.15 K in Table 3. The density (ρ), refractive index (n_D), surface tension (γ) and pH were fitted by least squares using the polynomial of second-order expression given by Eq. (1):

$$Z = A_0 + A_1 T(K) + A_2 T(K)^2 \quad (1)$$

Where Z is ρ (g•mL⁻¹), n_D , pH, or γ (mN•m⁻¹), T is the temperature (K), and A_0 , A_1 , and A_2 are the adjustable parameters.

The values of viscosities were fitted using the Eq. (2):

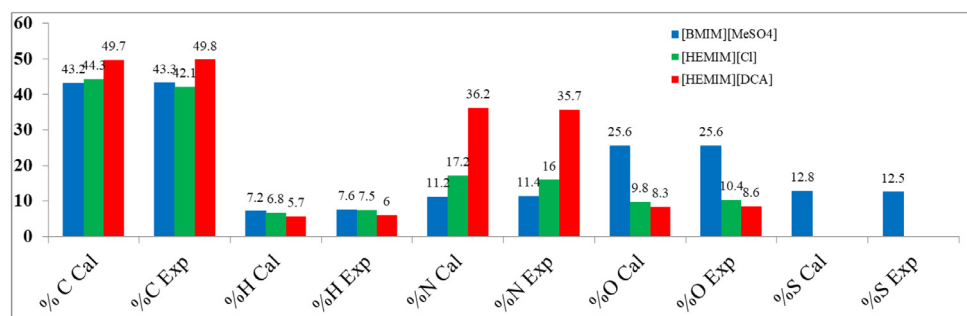
$$\ln \eta(mPa.s) = \frac{A_0}{T(K) - A_1} \quad (2)$$

Where A_0 and A_1 are adjustable parameters, and T is temperature. The best-fit parameters for density, refractive index, surface tension, and viscosity were listed in Table 4, together with their standard deviations (S.D.). The S.D. values were calculated by applying

Table 1

Characteristic absorption bands in the IR spectrum of the synthesized ILs.

ν , cm ⁻¹	[BMIM][MeSO ₄]	ν , cm ⁻¹	[HEMIM][Cl]	ν , cm ⁻¹	[HEMIM][DCA]
3526	Valence vibrations of N-H in (R)NH ₂ Valence vibrations of O-H in water (Overlapped)	3336	Valence vibrations of O-H	3318	Valence vibrations of O-H
2874	Valence vibrations of C-H in CH ₂ , CH ₃ , and (R)-CH ₃	1638	Valence vibrations of C=C Valence vibrations of C-H ring	2198–2240	Valence vibrations of C≡N
1572	Scissor-like deformational vibrations of N-H in (R)NH ₂ , NH ₂ ,	1571	Scissor-like deformational vibrations of N-H in (R)NH ₂ , NH ₂	1569	Scissor-like deformational vibrations of N-H in (R)NH ₂ , NH ₂
		1452	Deformation vibrations of NH ₃ ⁺ , NH ₂ ⁺ , NH ⁺ Valence vibrations of N = N in azo-compounds	1451	Deformation vibrations of NH ₃ ⁺ , NH ₂ ⁺ , NH ⁺ Valence vibrations of N = N in azo-compounds
1466	Deformation vibrations of NH ₃ ⁺ , NH ₂ ⁺ , NH ⁺ Valence vibrations of N = N in azo-compounds	1339	Stretch vibrations of C-C	1425–1450	Valence vibrations of CH ₂
1400–1000	Valence vibrations of N-C	1167	Cl ⁻	1316	Valence vibrations of C-C
1012–1029	Valence vibrations of S = O	1072	Valence vibrations of C-O	1073	Valence vibrations of C-O
1170	Deformation vibrations of CH ₃ groups linked to carboxyl groups; Valence vibrations of N-C	870	Stretch vibrations of CH ₂ -OH	869–906	Stretch vibrations of CH ₂ -OH
1059	Valence vibrations of C-C	760	Valence vibrations of C-H ring	753	Valence vibrations of C-H ring
738	Deformation vibrations of NH ₂	652–703	Valence vibrations of CH ₃ -N	651–703	Valence vibrations of CH ₃ -N
624–654	Vibrations of SO ₄ ²⁻	622	Valence vibrations of N-H	622	Valence vibrations of N-H

**Fig. 3.** The CHNOS elemental analysis for synthesized ILs.**Table 2**
Impurities of the synthesized ILs^a.

Species	Test Method	Results		
		[BMIM][MeSO ₄]	[HEMIM][Cl]	[HEMIM][DCA]
Water content, mass%	Karl Fischer	0.060	0.500	0.075
Chloride, mass%	Potentiometry	–	22.81	–
Bromide, ppm		<10	<10	<10
Sulfate, ppm	Turbidimetry	<5	<5	<5
Heavy metals (as Pb), ppm		<0.2	<0.2	<0.2
Ash content, mass%	Electric furnace and gravimetry	<0.001	<0.001	<0.001

^a Before use, the prepared ILs were treated by heating in a vacuum oven at ≈–0.1 MPa.

the Eq. (3):

$$SD = \left[\sum^{(z_{exp} - z_{cal})^2} / n \right]^{1/2} \quad (3)$$

Where z and n are the property values and the number of experimental points, respectively [6,50–52].

3.3. Density

The effects of temperature, cation, and anion type on the density of synthesized ILs were revealed in Table 3 and Fig. 4. As expected, the measured densities decreased as a function of temperature.

According to Fig. 4, it was found that the density was related to an anion in the order of decreasing molecular weight. The density of ILs was increased when anion molecular weight was amplified. The higher density values were due to the presence of more heteroatoms in comparison with other anions. The unexpectedly low density of [HEMIM][Cl], opposing to the lower molecular weight of its anion, might be owing to the presence of moisture and the symmetric nature of Cl⁻, which may result in the soft packing and a higher density. This observation and the literature reports [53–55] presented that in a series of ILs with common cation, the density behavior was an outcome of both the molecular weight and the symmetry elements associated with the constituent anions. To estimate the thermal expansion coefficients, the density values were used as a function of temperature with the following

Table 3

Density (ρ), dynamic viscosity (η), refractive index (n_D), surface tension (γ), conductivity (σ), speed of sound (u), pH and thermal expansion (α) of the ionic liquids at different temperatures.

T/(K)	ρ /(g mL ⁻¹)	η /(mPa.s)	n_D	γ /(mN m ⁻¹)	σ /(mS) (1% Solution)	pH (1% Solution)	u /(m s ⁻¹)	$\alpha^* 10^4$ /k ⁻¹
[BMIM][MeSO₄]								
283.15	1.2120	378.9	1.4830	45.6 ± 0.1	2.00	7.2	1604.36	4.182
293.15	1.2111	202.0	1.4794	44.5 ± 0.1	2.06	7.01	1579.15	4.265
298.15	1.2070	150.4	1.4785	44.0 ± 0.1	2.08	6.82	1570.70	4.308
303.15	1.2051	115.3	1.4759	43.8 ± 0.1	2.10	6.7	1567.56	4.350
313.15	1.1970	71.32	1.4743	42.6 ± 0.1	2.12	6.5	1545.57	4.436
323.15	1.1911	46.97	1.4720	42.0 ± 0.1	2.13	6.25	1536.01	4.523
333.15	1.1860	32.58	1.4700	41.2 ± 0.1	2.14	6.01	1520.68	4.611
343.15	1.1800	23.64	1.4674	40.0 ± 0.1	2.16	5.84	1495.88	4.701
353.15	1.1733	17.70	1.4658	39.7 ± 0.1	2.17	5.65	1494.04	4.790
363.15	1.1698	13.70	1.4631	39.0 ± 0.1	2.17	5.48	1479.27	4.882
[HEMIM][Cl]								
283.15	1.2231	445.6	1.5290	68.0 ± 0.1	4.15	6.35	2085.26	4.873
293.15	1.2175	213.8	1.5268	66.5 ± 0.1	4.19	6.19	2060.61	4.870
298.15	1.2147	154.8	1.5243	65.4 ± 0.1	4.21	6.05	2040.81	4.865
303.15	1.2118	114.4	1.5241	65.0 ± 0.1	4.23	5.92	2035.69	4.860
313.15	1.2063	67.75	1.5213	64.0 ± 0.1	4.32	5.68	2020.77	4.852
323.15	1.2010	43.10	1.5192	62.4 ± 0.1	4.36	5.47	1992.59	4.840
333.15	1.1956	29.14	1.5170	59.8 ± 0.1	4.38	5.20	1942.33	4.831
343.15	1.1902	20.72	1.5147	56.0 ± 0.1	4.40	5.00	1864.23	4.820
353.15	1.1849	15.38	1.5120	53.1 ± 0.1	4.43	4.79	1804.24	4.810
363.15	1.1795	11.78	1.5095	50.2 ± 0.1	4.45	4.58	1742.81	4.790
[HEMIM][DCA]								
283.15	1.1970	180.7	1.5332	63.4 ± 0.1	2.87	8.16	2018.49	5.030
293.15	1.1914	93.44	1.5329	62.0 ± 0.1	2.96	7.95	1994.73	5.072
298.15	1.1882	70.36	1.5308	61.5 ± 0.1	3.11	7.83	1987.50	5.092
303.15	1.1849	54.34	1.5287	60.2 ± 0.1	3.13	7.68	1962.85	5.110
313.15	1.1784	34.54	1.5249	57.7 ± 0.1	3.14	7.48	1914.80	5.151
323.15	1.1710	23.53	1.5233	56.2 ± 0.1	3.15	7.31	1889.21	5.201
333.15	1.1656	16.94	1.5202	54.5 ± 0.1	3.15	7.14	1856.40	5.240
343.15	1.1592	12.76	1.5164	53.2 ± 0.1	3.16	6.97	1833.32	5.291
353.15	1.1520	9.935	1.5141	52.4 ± 0.1	3.17	6.82	1822.37	5.330
363.15	1.1461	7.960	1.5110	51.5 ± 0.1	3.18	6.68	1807.51	5.381

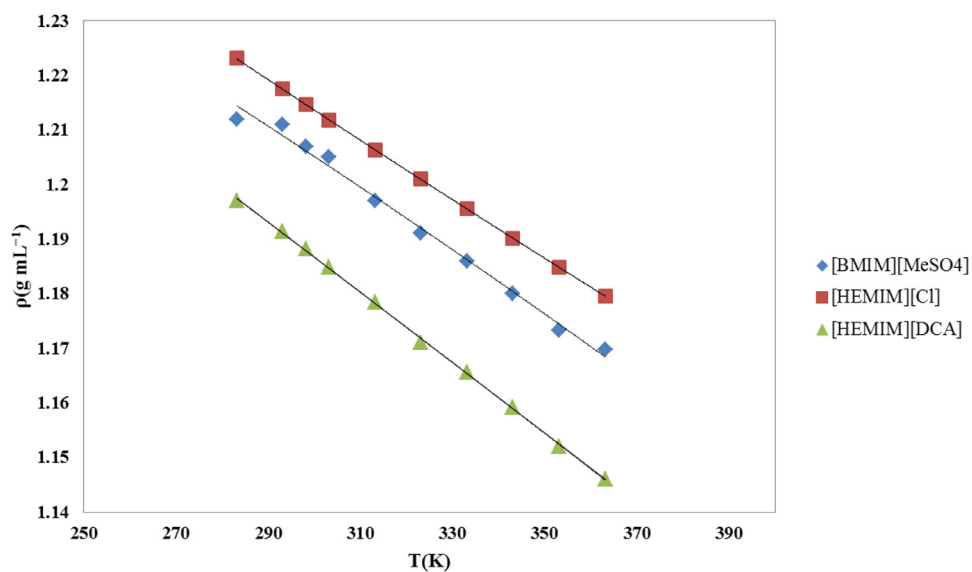


Fig. 4. The plot of density versus temperature for synthesized ILs.

equation:

$$\alpha = -\frac{1}{\rho} \left(\frac{\partial \rho}{\partial T} \right) = -(A_1 + 2A_2 \times T) / (A_0 + A_1 \times T + A_2 \times T^2) \quad (4)$$

where α is the coefficient of thermal expansion, ρ is the ILs density, and A_0 , A_1 , and A_2 are the adjustable parameters calculated in Eq. (1). The thermal expansion coefficients for each of ILs at several temperatures were summarized in Table 3. The results showed that

the variation of the volume expansivity quantified by the thermal expansion coefficient could be considered almost as independent of the temperature for these ILs.

Correspondingly, the density data of fluids were considered very informative, for it could be used to estimate other several important physical parameters like molecular/molar volume, standard molar entropy, and lattice energy. The parameters related to the fluids' bulk properties were expected to provide some useful

Table 4

Fitting parameters of Eqs. (1) and (2) and standard deviations in Eq. (3) used to correlate the physical properties of synthesized ionic liquids.

Physical property [BMIM][MeSO ₄]	A ₀	A ₁	A ₂	R ²	S.D.
ρ /(g mL ⁻¹)	1.3391	-0.0003	-4×10^{-7}	0.9915	0.0054
n_D	1.6247	-0.0007	7×10^{-7}	0.9949	0.0010
γ /(mN m ⁻¹)	94.913	-0.2457	-0.0003	0.9955	0.430
pH	19.753	-0.0673	6×10^{-5}	0.9985	0.0158
η /(mPa.s)	404.9297	-56.8642	-	0.9940	0.0913
[HEMIM][Cl]					
ρ /(g mL ⁻¹)	1.4007	-0.0007	2×10^{-7}	0.9999	0.0053
n_D	1.6022	-0.0003	6×10^{-8}	0.9967	0.0066
γ /(mN m ⁻¹)	62.691	0.99	-0.0019	0.9937	0.268
pH	14.115	-0.0308	10^{-5}	0.9987	0.0285
η /(mPa.s)	363.5655	-48.2585	-	0.9933	0.1053
[HEMIM][DCA]					
ρ /(g mL ⁻¹)	1.3682	-0.0006	-1×10^{-7}	0.9994	0.0052
n_D	1.5868	-0.0001	-3×10^{-7}	0.9913	0.0056
γ /(mN m ⁻¹)	196.4	-0.7082	0.0008	0.9921	0.458
pH	21.114	-0.0671	8×10^{-5}	0.9991	0.0474
η /(mPa.s)	301.1730	-46.7876	-	0.9947	0.0805

Table 5

Thermodynamic and equilibrium parameters viz., molecular volume (V_m), standard molar entropy (S°) and lattice energy (U_{pot}) (obtained at 298.15 K recorded for synthesized ILs).

ILs	V_m /nm ³	S° /J.K ⁻¹ .mol ⁻¹	U_{pot} /kJ.mol ⁻¹
[BMIM][MeSO ₄]	0.3443	458.7	438.5
[HEMIM][Cl]	0.2223	306.6	491.1
[HEMIM][DCA]	0.2700	366.1	466.8

insight into the structure-property relationships prevalent in RTILs. The molecular volume of any ionic compound, defined as the sum of ionic volumes (V_{ion}) of its constituent ions, served as an index of the ionic size [55,56]:

$$V_m = V(A^+) + V(X^-) \quad (5)$$

In contrast to the ionic radius, the ionic volumes were well defined and are valid for both symmetrical and asymmetrical ions. From the density data, the molecular volume (V_m in nm³) at 298.15 K of each IL was calculated using the Eq. (6) [55,57]:

$$V_m = \frac{M}{N_A \rho} \quad (6)$$

where M is molar mass, ρ is density, and N_A is Avogadro's constant. The calculated values of V_m were presented in Table 5. Using calculated V_m , ρ and molar mass of synthesized ILs, the standard molar entropy (S°) and lattice energy (U_{pot}) were calculated at 298.15 K for these fluids using Eqs. (7) and (8) [55,57,58]:

$$S^\circ(298.15K)/J.K^{-1}.mol^{-1} = 1246.5(V_m/nm^3) + 29.5 \quad (7)$$

$$U_{pot}(298.15K)/kJ.mol^{-1} = 1981.2(\rho/M)^{1/3} + 103.8 \quad (8)$$

The calculated values of S° and U_{pot} were also presented in Table 5. The lower lattice energy was the underlying reason for the instability of the solid phase of imidazolium-based ILs at normal temperatures.

3.4. Viscosity

The experimental data of ILs viscosity as a temperature function was shown in Table 4 and Fig. 5. As expected in Fig. 5, the viscosity of ILs significantly decreased with increasing temperature. According to Fig. 5, the order of viscosity was as follows: [HEMIM][Cl]>[BMIM][MeSO₄]> [HEMIM][DCA]. At high temperature, the movement of ILs molecules was much faster and freer; thus, the viscosity was reduced. A look into the published viscosity data for

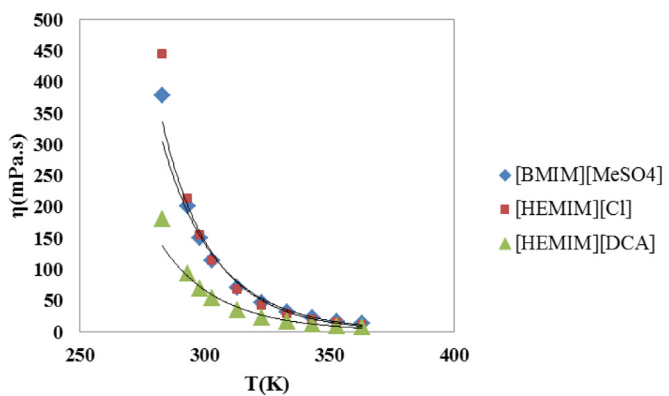


Fig. 5. Plot depicting the variation of viscosity as a function of temperature for synthesized ILs.

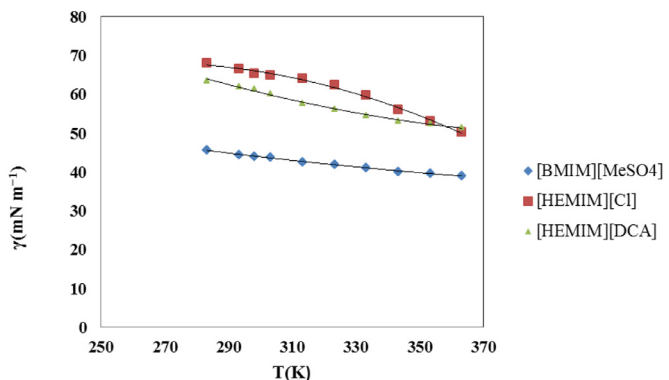


Fig. 6. Experimental values of surface tension γ (mN m⁻¹) against temperature (K) for synthesized ILs.

the ILs revealed that electrostatic interactions, hydrogen bonding, and van der Waals interactions were the main factors that decide the magnitude of viscosity [59,60]. Geometric aspects of the constituent ions have also been found to affect the viscosity of ILs significantly [61]. In this regard, the more planar structures result in lower viscosities as planarity allowed to easier slip between constituents. Besides, the symmetry and shape of the constituent ions of ILs have also been claimed to influence their viscosity behavior [36,62]. All these reasons could be justified by higher viscosity of [HEMIM][Cl].

3.5. Surface tension

Surface tension (γ) of liquids and its temperature dependence attended as reliable indices of their surface composition, structure, and thermodynamics. In fluid physics, the magnitude of γ was considered a measure of cohesive energy prevailing among the fluid constituents. To arrive at such information and the composition dependence of these characteristics, the γ values of the synthesized ILs were measured in the temperature range of 283.15 K to 363.15 K shown in Table 3 and Fig. 6. The measured surface tension for ILs was lower than water (71.9 mN•m⁻¹) and higher than most of the common organic solvents (ethanol: 21.9 mN•m⁻¹) [63]. According to Fig. 6, the surface tension values decreased with increasing temperature. The results indicated that the cation and anion of ILs affected surface tension since the cation and anion were present at the interface. Hence, both of them collaborated in surface energy [51,64]. The surface tension values followed the order: [HEMIM][Cl]> [HEMIM][DCA]> [BMIM][MeSO₄]. The high surface tension for [HEMIM][Cl] was due to hydrogen bonds' existence in these anions. In contrast, low surface tension in [HEMIM][DCA]

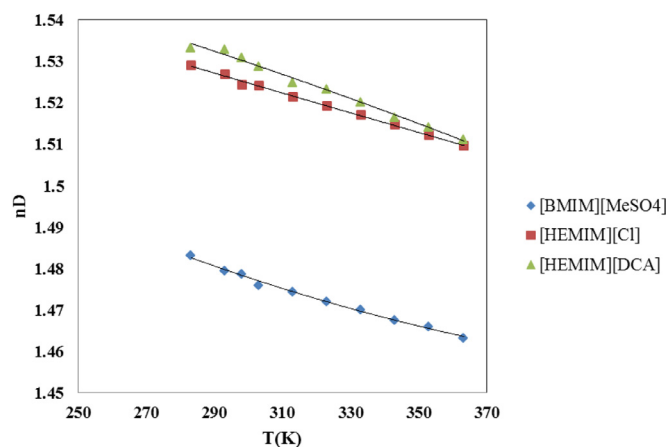


Fig. 7. Experimental values of refractive index n_D , against temperature (K) for synthesized ILs.

and $[\text{BMIM}][\text{MeSO}_4]$ could be attributed to the possibility of higher charge delocalization in their anions, leading to their weaker electrostatic interactions with the imidazolium cations.

3.6. Refractive index and pH

The refractive index of a compound indicated the ability of light reflection, which entered the medium. A high refractive index is considered greater than 1.4 for a substance above the most common organic materials. Therefore, the greater the refractive index of a compound, the more refracted light. The refractive index was an important factor for defining the purity and electronic polarizability of ionic liquids. Table 3 and Fig. 7 showed the temperature dependence of the refractive index for the studied ILs. In all the cases, values were found higher than 1.4. The refractive index linearly decreased with increasing the temperature. Increasing trend of refractive index for studied ILs was as follows: $[\text{HEMIM}][\text{DCA}] > [\text{HEMIM}][\text{Cl}] > [\text{BMIM}][\text{MeSO}_4]$. It could be said that the high refractive index of the $[\text{HEMIM}][\text{DCA}]$ was due to the asymmetric structure of this IL, which cannot be close-packed in microscopic structure.

The measured pH values of 1% aqueous ionic liquids solution were presented as a function of temperature in Table 3 and Fig. 8. As can be seen, the pH change was low when the temperature was increased. It can be said that the pH of the studied ionic liquids in the wide range of temperatures was almost constant. The studied ILs included alkali and acidic ionic liquids in the pH range of 4 to 8. It was necessary to measure ionic liquids' pH values for their unique application in the chemical, petroleum, and pharmaceutical industries.

3.7. Conductivity

Table 3 also included the conductivity (σ) data of 1% aqueous ionic liquids solution at varying temperatures. The differences between the conductivity can be explained by the interaction strength between cation and anion, the ion volumes, and steric effects affecting these volumes. Fig. 9 showed the temperature dependence of electrical conductivity for the ILs studied. At a wide range of temperatures, $[\text{HEMIM}][\text{Cl}]$ had a maximum electrical conductivity. As mentioned, less unpaired ions would be responsible for the current transport, so in $[\text{HEMIM}][\text{Cl}]$, we observed the weakest interaction between anion and cation.

3.8. Speed of sound

The speed of sound, u , as a valuable thermodynamic property could be experimentally determined with great precision over a broad range of temperature and pressure. It might be related to other thermodynamic properties such as density, heat capacity, thermal conductivity, and isentropic and isothermal compressibilities, which were essential for the final design and optimization of several industrial processes [65,66]. Several research [67–69] tried to obtain calculated values of sound speed for ILs by theoretical and empirical formulas, such as Auerbach's equation. Auerbach's equation [70,71] was a well-known empirical relation between the speed of sound (u), surface tension (γ), and density (ρ) of liquids:

$$u = \left(\frac{\gamma}{6.33 \times 10^{-10} * \rho} \right)^a \quad (9)$$

where a is equal to 2.3, u is the speed of sound in $\text{m} \cdot \text{s}^{-1}$, γ is the surface tension in $\text{N} \cdot \text{m}^{-1}$, and ρ is the density in $\text{kg} \cdot \text{m}^{-3}$. Gardas and Coutinho [69] showed that the original version of Auerbach's equation could not be used to direct-prediction of the sound speed for imidazolium-based ILs. They proposed a modified version of Auerbach's relation with $a = 0.671460 \pm 0.0002$ in Eq. (9).

Calculated values of sound speed (from Eq. (9)) for the studied ILs as a function of temperature were given in Table 3. As we can see, the sound speed decreased with an increase in temperature for the investigated ILs. In all temperature ranges, $[\text{HEMIM}][\text{Cl}]$ showed the highest sound velocity, which might be due to the highest surface tension between the synthesized ionic liquids.

3.9. Thermal stability

Data on the thermal behavior of synthesized ionic liquids was required to obtain thermal stability information for their use in the chemical process, development of contacting equipment, and storage conditions [72–74]. Thermal analysis showed an important role in the characterization and determination of the thermal stability of novel materials such as ionic liquids [75–77]. Therefore, the thermal properties of the investigated ionic liquids have been characterized by TG/DTG techniques. Thermograms of the studied ILs, ($[\text{BMIM}][\text{MeSO}_4]$, $[\text{HEMIM}][\text{Cl}]$ and $[\text{HEMIM}][\text{DCA}]$) were shown in Fig. 10.

The TGA/DTG curves of $[\text{BMIM}][\text{MeSO}_4]$ disclosed no thermal event before 573 K, which confirmed that this ionic liquid would be thermally stable in the temperature range of 298–573 K. Above this temperature, TGA/DTG curve was observed with an endothermic phenomenon at the temperature range of about 583–773 K, which it might have corresponded to the thermal decomposition of $[\text{BMIM}][\text{MeSO}_4]$. In the TGA/DTG curve of $[\text{HEMIM}][\text{Cl}]$, it was shown that this ionic liquid was thermally stable up to about 523 K. However, at higher temperatures, TGA/DTG curves for $[\text{HEMIM}][\text{Cl}]$ presented a significant mass loss step between 533 and 773 K. As it is evident from the TGA/DTG curves of $[\text{HEMIM}][\text{DCA}]$, a principal thermal decomposition occurred above 473 K, where the ionic liquid sample showed an endothermic decomposition. Such a thermal pattern suggested that $[\text{HEMIM}][\text{DCA}]$ was thermally stable until 473 K. However, a maximum mass loss was perceived in the temperature of about 493 K. The thermoanalytical data for the studied ionic liquids in this investigation exhibited the following thermal stability order: $[\text{BMIM}][\text{MeSO}_4] > [\text{HEMIM}][\text{Cl}] > [\text{HEMIM}][\text{DCA}]$.

3.10. Electrochemical window

The electrochemical window was defined as the potential interval observed between the reduction potential of the organic

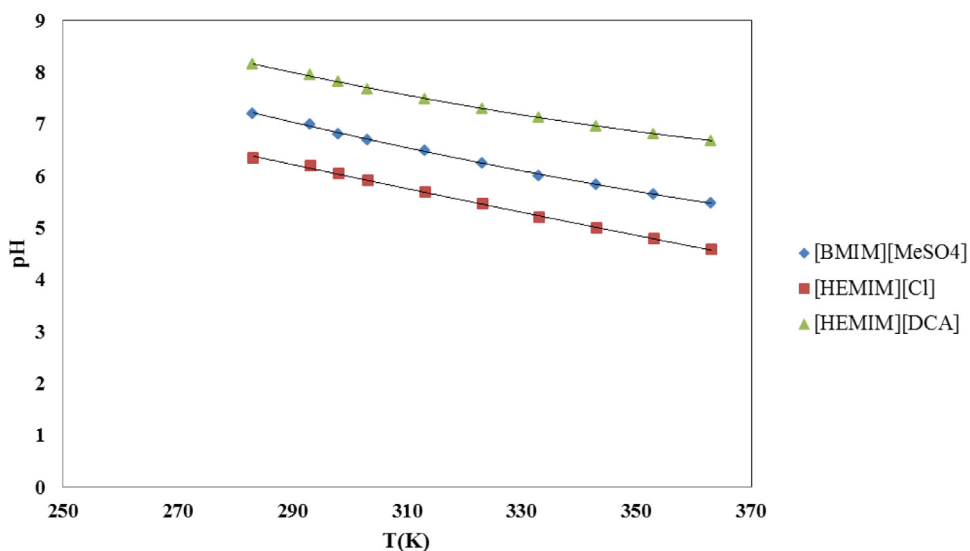


Fig. 8. Experimental values of pH against temperature (K) for synthesized IL.

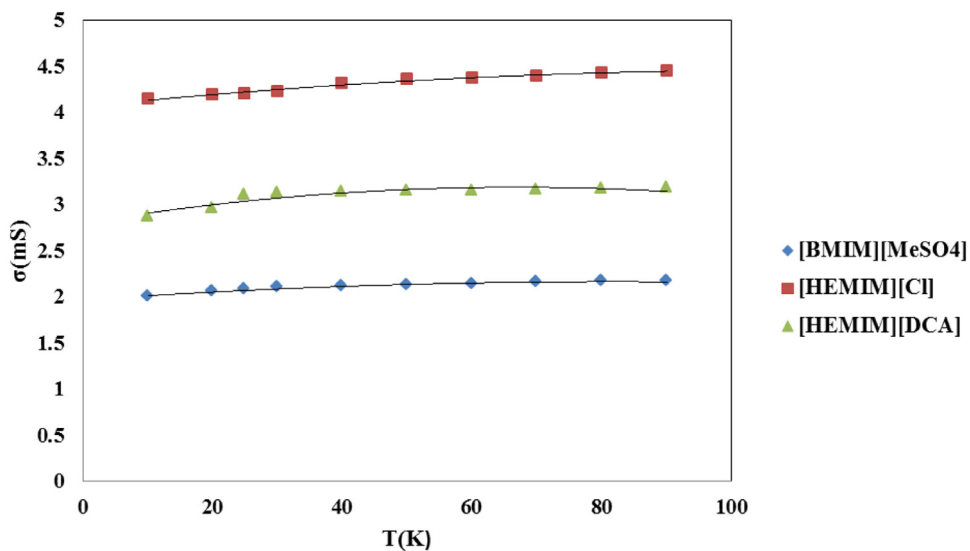


Fig. 9. Experimental electrical conductivity (σ) as a function of temperature for synthesized ILs.

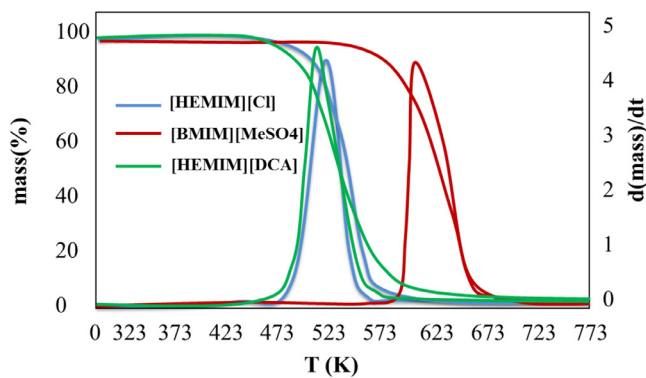


Fig. 10. TGA and DTG curves for the three prepared ionic liquids at the heating rate of 10 K min⁻¹.

cationic part and the oxidation potential of the anionic part of pure ILs. A wide electrochemical window made ILs as promising electrolytes for electrochemical power applications. Most ILs possessed

a wide potential window of >4.0 V. It has been found that, for some ionic liquids, the potential of anode limit proportionally decreased with increasing the highest occupied molecular orbit energy calculated for the anion [78,79]. In this work, the electrochemical windows of the investigated ILs were experimentally obtained using cyclic voltammetric analyses at SP-GCE and using Ag wire as a quasi-reference electrode, as shown in Fig. 11. As can be seen, the electrochemical windows for the ILs studied ranged from about 4 V to 6 V, and decreased in the following order: [BMIM][MeSO₄] > [HEMIM][DCA] > [HEMIM][Cl].

It was noteworthy that some nonaqueous solvents such as DMSO, AN, DMF, etc. were available for H₂S and thiols' voltammetric study. Still, they were often toxic and weakly conductive so that they needed to use the supporting electrolyte to provide enough conductivity in the solution. Also, other disadvantages of the existing standard methods e.g. UOP-163 used for this purpose, were mentioned. Our synthesized ILs were pure fluids with unique properties of excellent conductivity and good solubility toward most organic materials. Thus studied ILs plays the role of both solvent and supporting electrolyte simultaneously in the electrochemical systems. So quantitative experiments were performed to evaluate

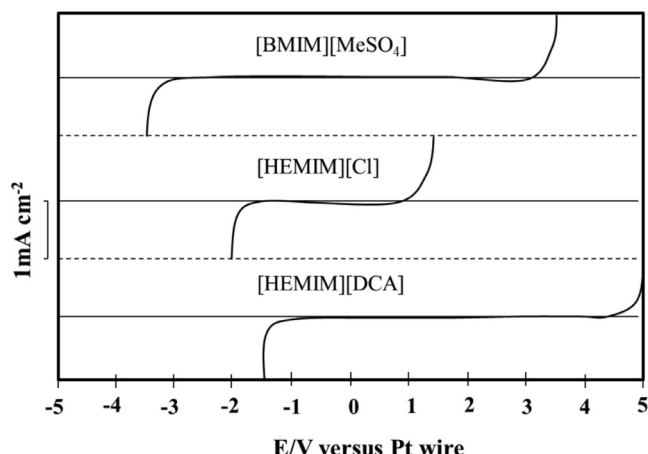


Fig. 11. Cyclic voltammograms of the purified tested ionic liquids. Conditions: quasi reference electrode, Ag wire; working electrode, SP-GCE (O.D. 2.2 mm); temperature, 298.15 K; scan rate, 100 mV s⁻¹.

the method for concurrent analysis of the H₂S and -SH group in the prepared ionic liquids. The developed technique, however, is a sensitive and selective square wave voltammetric (SWV) approach, which needs a single drop of the sample for test. It is noteworthy that all voltammetric experiments were performed at a holding time of 10 to 60 s. Due to ionic liquids' chemical stability, no significant change in cyclic voltammograms was achieved during this time interval. Therefore, a holding time of 10 s was selected for all samples and voltammograms were recorded at this holding time. The resulting voltammogram obtained for H₂S and R-SH in pure ILs prepared through SP-GCE can be seen in Fig. 12.

As shown in Fig. 12 in all studied ILs we observed recognizable individual reversible peaks due to the oxidation of H₂S and

ethanethiol, although our analyses were electroactive. Also, the detection of H₂S on all three synthesized ILs was better than that of thiol, which could be attributed to stronger hydrogen bonding and less steric hindrance. The mechanism envisaged for this process was the mechanism of "Michael reaction" or "Michael addition," which was a justification for the superiority of H₂S uptake over thiol. In fact, with this, "reactive" ionic liquids were reported here that were capable of reacting with thiols and hydrogen sulfide entirely via a reversible Michael addition to producing non-volatile ionic matrices with attached "odorous" segments [80,81]. On the other hand, as we have seen, the best medium among these mentioned ionic liquids that were used to separate RSH and H₂S was [BMIM][MeSO₄], which was due to hydrophobic property and electrochemical stability as a solvent for organic and even inorganic compounds. Also, thiol(H₂S)-ILs anion interactions were mainly due to weak dispersive forces and the dependency behavior with the anions nature strongly ensues from their polarity, so [BMIM][MeSO₄] due to the presence of [MeSO₄] anion compared to other ionic liquids was a better environment for the removal of sulfur compounds [82].

Table 6 was also listed in the comparison of this research work with the available references. It was noteworthy that no report has been published so far for [HEMIM][DCA] and [HEMIM][CL]. Therefore, for the first time, these ionic liquids' physicochemical properties were measured and reported in the wide range of temperatures in this research work. In Table 6, only some comparative results of [BMIM][MeSO₄] were compiled.

4. Conclusion

The data of physicochemical properties on ionic liquids were critical for both theoretical research and industrial application. Creating a database would develop research and investigation of ionic liquids. Thus, here, for the first time, we synthesized,

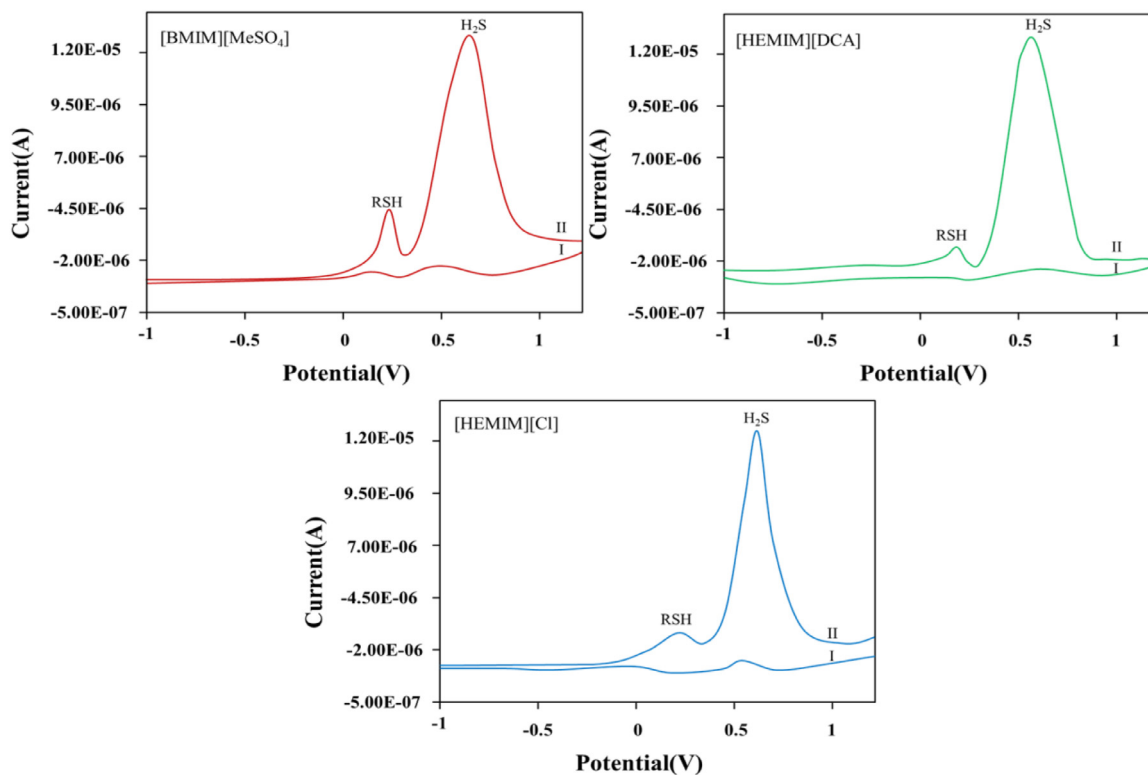


Fig. 12. Typical SWV voltammogram of I) Pure ILs [Blank samples] II) 10 µg g⁻¹ thiol and 100 µg g⁻¹ sulfide ion in the investigated ionic liquids; working electrode, SP-GCE (O.D. 2.2 mm); temperature, 298.15 K; scan rate, 100 mV s⁻¹ holding time 10 s.

Table 6

Experimental and literature values of densities (ρ), refractive indices (n_D), dynamic viscosities (η), surface tensions (γ) of the [BMIM][MeSO₄] at 293.15, 298.15 and 303.15 K.

property	Present work			Literature		
	293.15 K	298.15 K	303.15 K	293.15 K	298.15 K	303.15 K
ρ /(g mL ⁻¹)	1.2111	1.2070	1.2051	1.2112 [5] 1.2117 [55]	1.2078 [5] 1.2084 [55]	1.2044 [5] 1.2050 [55]
η /(mPa.s)	202.0	150.4	115.3	269.1 [52] – 122.3 [37]	209.0 [55] 93.78 [37]	151.9 [52] 169 [55] 73.35 [37]
n_D	1.4794	1.4785	1.4759	1.4804 [52] –	– 1.4782 [83]	1.4781 [52] 1.4770 [83]
γ /(mN m ⁻¹)	44.5	44.0	43.8	45.5 [55] 44.1 [84] 44.4 [37]	45.1 [55] 43.3 [84] 43.7 [37]	44.8 [55] 42.8 [84] 43.4 [37]

characterized, and carefully measured several essential properties of ionic liquids 1-butyl-3-methylimidazolium methyl sulfate, 1-(2-Hydroxyethyl)-3-methylimidazolium chloride, and 1-(2-Hydroxyethyl)-3-methylimidazolium dicyanamide in the wide temperature range. Because of the inherent advantages of these ILs, such as a scavenger for some environmental pollutants (i.e., hydrogen sulfide), and for objectives in our further researches, we considered studying density, viscosity, surface tension, refractive index, pH, conductivity, speed of sound, thermal expansion. Also, the thermal stability and electrochemical window of these ILs were accurately measured. The results showed that these physicochemical properties quite temperature depended, and anion of ILs affected them. The results also showed that, by using square wave voltammetry, synthesized ILs are the best medium for the simultaneous determination of RSH and H₂S.

Declaration of Competing Interest

The authors declare that they have no known competing financial interests or personal relationships that could have appeared to influence the work reported in this paper.

CRediT authorship contribution statement

Seyed Mohammad Reza Shoja: Conceptualization, Writing - original draft, Writing - review & editing, Validation. **Majid Abdouss:** Supervision, Conceptualization, Validation, Writing - review & editing. **Ali Akbar Miran Beigi:** Resources, Formal analysis.

References

- [1] I.A. Lawal, M. Klink, P. Ndungu, B. Moodley, Brief bibliometric analysis of "ionic liquid" applications and its review as a substitute for common adsorbent modifier for the adsorption of organic pollutants, Environ. Res. (2019).
- [2] T.J. Szalaty, Ł. Kłapiszewski, T. Jesionowski, Recent developments in modification of lignin using ionic liquids for the fabrication of advanced materials-A review, J. Mol. Liq. (2020) 112417.
- [3] V.L. Martins, R.M. Torresi, Ionic liquids in electrochemical energy storage, Curr. Opin. Electrochem. 9 (2018) 26–32.
- [4] P. Halder, S. Kundu, S. Patel, A. Setiawan, R. Atkin, R. Parthasarthy, J. Paz-Ferreiro, A. Surapaneni, K. Shah, Progress on the pre-treatment of lignocellulosic biomass employing ionic liquids, Renew. Sustain. Energy Rev. 105 (2019) 268–292.
- [5] F. Yebra, K. Zemánková, J. Troncoso, Speed of sound in ionic liquids with a common ion as a function of pressure and temperature, J. Chem. Thermodyn. 116 (2018) 235–240.
- [6] M. Yousefi, M. Abdouss, A.A.M. Beigi, A. Naseri, Synthesis and characterization of physicochemical properties of hydrophilic imidazolium-based ionic liquids, Korean J. Chem. Eng. 34 (9) (2017) 2527–2535.
- [7] I. Pacheco-Fernández, V. Pino, Green solvents in analytical chemistry, Curr. Opin. Green Sustain. Chem. 18 (2019) 42–50.
- [8] J.M. Rieland, B.J. Love, Ionic liquids: a milestone on the pathway to greener recycling of cellulose from biomass, Resour. Conserv. Recycl. 155 (2020) 104678.
- [9] B. Aghabarari, M. Ghiaci, S.G. Amini, E. Rahimi, M. Martinez-Huerta, Esterification of fatty acids by new ionic liquids as acid catalysts, J. Taiwan Inst. Chem. Eng. 45 (2) (2014) 431–435.
- [10] S. Zeng, X. Zhang, L. Bai, X. Zhang, H. Wang, J. Wang, D. Bao, M. Li, X. Liu, S. Zhang, Ionic-liquid-based CO₂ capture systems: structure, interaction and process, Chem. Rev. 117 (14) (2017) 9625–9673.
- [11] L. Brown, M.J. Earle, M.A. Gilea, N.V. Plechikova, K.R. Seddon, in: Ionic Liquid-Liquid Chromatography: A New General Purpose Separation Methodology, Ionic Liquids II, Springer, 2017, pp. 85–125.
- [12] K. Wang, H. Adidharma, M. Radosz, P. Wan, X. Xu, C.K. Russell, H. Tian, M. Fan, J. Yu, Recovery of rare earth elements with ionic liquids, Green Chem. 19 (19) (2017) 4469–4493.
- [13] R. Alayoubi, N. Mehmood, E. Husson, A. Kouzayha, M. Tabcheh, L. Chaveriat, C. Sarazin, I. Gosselin, Low temperature ionic liquid pretreatment of lignocellulosic biomass to enhance bioethanol yield, Renew. Energy 145 (2020) 1808–1816.
- [14] Z. Usmani, M. Sharma, P. Gupta, Y. Karpichev, N. Gathergood, R. Bhat, V.K. Gupta, Ionic liquid based pretreatment of lignocellulosic biomass for enhanced biocorversion, Bioresour. Technol. (2020) 123003.
- [15] S.M. Salman, S. Narayanaperumal, R.S. Schwab, C.R. Bender, O.E. Rodrigues, L. Dornelles, CuO nano particles and [bmim] BF 4: an application towards the synthesis of chiral β -seleno amino derivatives via ring opening reaction of aziridines with diorganyl diselenides, RSC Adv. 2 (22) (2012) 8478–8482.
- [16] I.M. Gindri, C.P. Frizzo, C.R. Bender, A.Z. Tier, M.A. Martins, M.A. Villetti, G. Machado, L.C. Rodriguez, D.C. Rodrigues, Preparation of TiO₂ nanoparticles coated with ionic liquids: a supramolecular approach, ACS Appl. Mater. Interfaces 6 (14) (2014) 11536–11543.
- [17] R.L. Vekariya, A review of ionic liquids: applications towards catalytic organic transformations, J. Mol. Liq. 227 (2017) 44–60.
- [18] M.S. Bin Dahbag, M.E. Hossain, A.A. AlQuaisra, Efficiency of ionic liquids as an enhanced oil recovery chemical: simulation approach, Energy Fuels 30 (11) (2016) 9260–9265.
- [19] A. Bera, J. Agarwal, M. Shah, S. Shah, R.K. Vij, Recent advances in ionic liquids as alternative to surfactants/chemicals for application in upstream oil industry, J. Ind. Eng. Chem. (2019).
- [20] Y. Hou, Y. Ren, W. Peng, S. Ren, W. Wu, Separation of phenols from oil using imidazolium-based ionic liquids, Ind. Eng. Chem. Res. 52 (50) (2013) 18071–18075.
- [21] K.S. Egorova, V.P. Ananikov, Fundamental importance of ionic interactions in the liquid phase: a review of recent studies of ionic liquids in biomedical and pharmaceutical applications, J. Mol. Liq. 272 (2018) 271–300.
- [22] M. Smiglak, J.M. Pringle, X. Lu, L. Han, S. Zhang, H. Gao, D.R. Macfarlane, R.D. Rogers, Ionic liquids for energy, materials, and medicine, Chem. Commun. 50 (66) (2014) 9228–9250.
- [23] S. Isikli, K.M. Ryan, Recent advances in solid-state polymer electrolytes and innovative ionic liquids based polymer electrolyte systems, Curr. Opin. Electrochem. (2020).
- [24] Z. He, P. Alexandridis, Ionic liquid and nanoparticle hybrid systems: emerging applications, Adv. Colloid Interface Sci. 244 (2017) 54–70.
- [25] J.P. Hallett, T. Welton, Room-temperature ionic liquids: solvents for synthesis and catalysis, 2, Chem. Rev. 111 (5) (2011) 3508–3576.
- [26] Q. Zhao, H. Chu, B. Zhao, Z. Liang, L. Zhang, Y. Zhang, Advances of ionic liquids-based methods for protein analysis, TRAC Trends Anal. Chem. 108 (2018) 239–246.
- [27] X. Yan, S. Anguille, M. Bendahan, P. Moulin, Ionic liquids combined with membrane separation processes: a review, Sep. Purif. Technol. (2019).
- [28] B. Sasikumar, G. Arthanareeswaran, A. Ismail, Recent progress in ionic liquid membranes for gas separation, J. Mol. Liq. 266 (2018) 330–341.
- [29] Y. Huang, Y. Zhang, H. Xing, Separation of light hydrocarbons with ionic liquids: a review, Chin. J. Chem. Eng. (2019).
- [30] J. Haider, S. Saeed, M.A. Qyyum, B. Kazmi, R. Ahmad, A. Muhammad, M. Lee, Simultaneous capture of acid gases from natural gas adopting ionic liquids: challenges, recent developments, and prospects, Renew. Sustain. Energy Rev. 123 (2020) 109771.
- [31] J.-L. Wang, L.-L. Wang, R.-J. Feng, Y. Zhang, Synthesis and characterization of novel anion exchange membranes containing bi-imidazolium-based ionic liquid for alkaline fuel cells, Solid State Ion. 278 (2015) 144–151.

- [32] S. Singhal, S. Agarwal, M. Singh, S. Rana, S. Arora, N. Singhal, Ionic liquids: green catalysts for alkene-isoalkane alkylation, *J. Mol. Liq.* (2019).
- [33] Z. Ullah, A.S. Khan, N. Muhammad, R. Ullah, A.S. Alqahtani, S.N. Shah, O.B. Ghaneem, M.A. Bustam, Z. Man, A review on ionic liquids as perspective catalysts in transesterification of different feedstock oil into biodiesel, *J. Mol. Liq.* 266 (2018) 673–686.
- [34] M. Díaz, A. Ortiz, I. Ortiz, Progress in the use of ionic liquids as electrolyte membranes in fuel cells, *J. Memb. Sci.* 469 (2014) 379–396.
- [35] X. Zhang, L. Pan, L. Wang, J.-J. Zou, Review on synthesis and properties of high-energy-density liquid fuels: hydrocarbons, nanofluids and energetic ionic liquids, *Chem. Eng. Sci.* 180 (2018) 95–125.
- [36] M. Shamsipur, A.A.M. Beigi, M. Tehmouri, S.M. Pourmortazavi, M. Iran-doust, Physical and electrochemical properties of ionic liquids 1-ethyl-3-methylimidazolium tetrafluoroborate, 1-butyl-3-methylimidazolium trifluoromethanesulfonate and 1-butyl-1-methylpyrrolidinium bis (trifluoromethylsulfonyl) imide, *J. Mol. Liq.* 157 (1) (2010) 43–50.
- [37] A.A.M. Beigi, M. Abdouss, M. Yousefi, S.M. Pourmortazavi, A. Vahid, Investigation on physical and electrochemical properties of three imidazolium based ionic liquids (1-hexyl-3-methylimidazolium tetrafluoroborate, 1-ethyl-3-methylimidazolium bis (trifluoromethylsulfonyl) imide and 1-butyl-3-methylimidazolium methylsulfate), *J. Mol. Liq.* 177 (2013) 361–368.
- [38] A. Jordan, N. Gathergood, Biodegradation of ionic liquids—a critical review, *Chem. Soc. Rev.* 44 (22) (2015) 8200–8237.
- [39] J. Hekayati, A. Roosta, J. Javanmardi, On the prediction of the vapor pressure of ionic liquids based on the principle of corresponding states, *J. Mol. Liq.* 225 (2017) 118–126.
- [40] Y. Guo, Z. Chen, Y. Zuo, Y. Chen, W. Yang, B. Xu, Ionic liquids with two typical hydrophobic anions as acidic corrosion inhibitors, *J. Mol. Liq.* 269 (2018) 886–895.
- [41] R.L. Gardas, H.F. Costa, M.G. Freire, P.J. Carvalho, I.M. Marrucho, I.M. Fonseca, A.G. Ferreira, J.A. Coutinho, Densities and derived thermodynamic properties of imidazolium-, pyridinium-, pyrrolidinium-, and piperidinium-based ionic liquids, *J. Chem. Eng. Data* 53 (3) (2008) 805–811.
- [42] E. Alcalde, I. Dinarès, A. Ibáñez, N. Mesquida, A simple halide-to-anion exchange method for heteroaromatic salts and ionic liquids, *Molecules* 17 (4) (2012) 4007–4027.
- [43] G. Appetecchi, M. Montanino, S. Passerini, Ionic liquid-based electrolytes for high energy, safer lithium batteries, *Ion. Liq. ACS Publ.* (2012) 67–128.
- [44] I. Dinarès, C.G. de Miguel, A. Ibáñez, N. Mesquida, E. Alcalde, Imidazolium ionic liquids: a simple anion exchange protocol, *Green Chem.* 11 (10) (2009) 1507–1510.
- [45] S. Peleteiro, S. Rivas, J.L. Alonso, V. Santos, J.C. Parajo, Utilization of ionic liquids in lignocellulose biorefineries as agents for separation, derivatization, fractionation, or pretreatment, *J. Agric. Food Chem.* 63 (37) (2015) 8093–8102.
- [46] L. Xue, E. Gurung, G. Tamas, Y.P. Koh, M. Shadeck, S.L. Simon, M. Maroncelli, E.L. Quitevis, Effect of alkyl chain branching on physicochemical properties of imidazolium-based ionic liquids, *J. Chem. Eng. Data* 61 (3) (2016) 1078–1091.
- [47] K.S. Quraishi, M.A. Bustam, S. Krishnan, M.I. Khan, C.D. Wilfred, J.-M. Lévéque, Thermokinetics of alkyl methylpyrrolidinium [NTf₂] ionic liquids, *J. Therm. Anal. Calorim.* 129 (1) (2017) 261–270.
- [48] D. Zheng, L. Dong, W. Huang, X. Wu, N. Nie, A review of imidazolium ionic liquids research and development towards working pair of absorption cycle, *Renew. Sustain. Energy Rev.* 37 (2014) 47–68.
- [49] H. Sulfide, in: *Mercaptan Sulfur in Liquid Hydrocarbons By Potentiometric Titration*, ASTM International, West Conshohocken, PA, 2010, p. 163. 10.
- [50] A. Pereiro, E. Tojo, A. Rodriguez, J. Canosa, J. Tojo, Properties of ionic liquid HMIMPF₆ with carbonates, ketones and alkyl acetates, *J. Chem. Thermodyn.* 38 (6) (2006) 651–661.
- [51] L.G. Sanchez, J.R. Espel, F. Onink, G.W. Meindersma, A.B.d. Haan, Density, viscosity, and surface tension of synthesis grade imidazolium, pyridinium, and pyrrolidinium based room temperature ionic liquids, *J. Chem. Eng. Data* 54 (10) (2009) 2803–2812.
- [52] E. Rodil, A. Arce Jr, A. Arce, A. Soto, Measurements of the density, refractive index, electrical conductivity, thermal conductivity and dynamic viscosity for tributylmethylphosphonium and methylsulfate based ionic liquids, *Thermochim. Acta* 664 (2018) 81–90.
- [53] C. Kolbeck, T. Cremer, K. Lovelock, N. Paape, P. Schulz, P. Wasserscheid, F. Maier, H.-P. Steinrück, Influence of different anions on the surface composition of ionic liquids studied using ARXPS, *J. Phys. Chem. B* 113 (25) (2009) 8682–8688.
- [54] M.P. Singh, S.K. Mandal, Y.L. Verma, A.K. Gupta, R.K. Singh, S. Chandra, Viscoelastic, surface, and volumetric properties of ionic liquids [BMIM][OcSO₄], [BMIM][PF₆], and [EMIM][MeSO₃], *J. Chem. Eng. Data* 59 (8) (2014) 2349–2359.
- [55] S.A. Pandit, M.A. Rather, S.A. Bhat, G.M. Rather, M.A. Bhat, Influence of the anion on the equilibrium and transport properties of 1-butyl-3-methylimidazolium based room temperature ionic liquids, *J. Solution Chem.* 45 (12) (2016) 1641–1658.
- [56] J.M. Slattery, C. Dagueret, P.J. Dyson, T.J. Schubert, I. Krossing, How to predict the physical properties of ionic liquids: a volume-based approach, *Angew. Chem. Int. Ed.* 46 (28) (2007) 5384–5388.
- [57] Q.-S. Liu, J. Tong, Z.-C. Tan, U. Welz-Biermann, J.-Z. Yang, Density and surface tension of ionic liquid [C₂mim][PF₃] (CF₂C_F₃) 3] and prediction of properties [C_nmim][PF₃] (CF₂C_F₃) 3](n= 1, 3, 4, 5, 6), *J. Chem. Eng. Data* 55 (7) (2010) 2586–2589.
- [58] W. Guan, X.-X. Ma, L. Li, J. Tong, D.-W. Fang, J.-Z. Yang, Ionic parachor and its application in acetic acid ionic liquid homologue 1-alkyl-3-methylimidazolium acetate {[C_nmim][OAc]}(n= 2, 3, 4, 5, 6), *J. Phys. Chem. B* 115 (44) (2011) 12915–12920.
- [59] G. Yu, D. Zhao, L. Wen, S. Yang, X. Chen, Viscosity of ionic liquids: database, observation, and quantitative structure-property relationship analysis, *AlChE J.* 58 (9) (2012) 2885–2899.
- [60] M. Moosavi, F. Khashei, A. Sharifi, M. Mirzaei, Transport properties of short alkyl chain length dicationic ionic liquids- the effects of alkyl chain length and temperature, *Ind. Eng. Chem. Res.* 55 (33) (2016) 9087–9099.
- [61] S. Seki, T. Kobayashi, Y. Kobayashi, K. Takei, H. Miyashiro, K. Hayamizu, S. Tsuzuki, T. Mitsugi, Y. Umebayashi, Effects of cation and anion on physical properties of room-temperature ionic liquids, *J. Mol. Liq.* 152 (1–3) (2010) 9–13.
- [62] A. Yadav, A. Guha, A. Pandey, M. Pal, S. Trivedi, S. Pandey, Densities and dynamic viscosities of ionic liquids having 1-butyl-3-methylimidazolium cation with different anions and bis (trifluoromethylsulfonyl) imide anion with different cations in the temperature range (283.15 to 363.15) K, *J. Chem. Thermodyn.* 116 (2018) 67–75.
- [63] N.-n. Ren, Y.-h. Gong, Y.-z. Lu, H. Meng, C.-x. Li, Surface tension measurements for seven imidazolium-based dialkylphosphate ionic liquids and their binary mixtures with water (methanol or ethanol) at 298.15 K and 1 atm, *J. Chem. Eng. Data* 59 (2) (2014) 189–196.
- [64] N. Naziri, R. Khordad, G. Rezaei, Effect of potential attraction term on surface tension of ionic liquids, *Physica B* 533 (2018) 50–57.
- [65] A. Queimada, J. Coutinho, I. Marrucho, J.-L. Daridon, Corresponding-states modeling of the speed of sound of long-chain hydrocarbons, *Int. J. Thermophys.* 27 (4) (2006) 1095–1109.
- [66] M.P. Singh, R.K. Singh, Correlation between ultrasonic velocity, surface tension, density and viscosity of ionic liquids, *Fluid Phase Equilib.* 304 (1–2) (2011) 1–6.
- [67] U. Domańska, K. Skiba, M. Zawadzki, K. Paduszyński, M. Królikowski, Synthesis, physical, and thermodynamic properties of 1-alkyl-cyanopyridinium bis [(trifluoromethyl) sulfonyl] imide ionic liquids, *J. Chem. Thermodyn.* 56 (2013) 153–161.
- [68] Q.-S. Liu, M. Yang, P.-F. Yan, X.-M. Liu, Z.-C. Tan, U. Welz-Biermann, Density and surface tension of ionic liquids [C_npy][NTf₂](n= 2, 4, 5), *J. Chem. Eng. Data* 55 (11) (2010) 4928–4930.
- [69] R.L. Gardas, J.A. Coutinho, Estimation of speed of sound of ionic liquids using surface tensions and densities: a volume based approach, *Fluid Phase Equilib.* 267 (2) (2008) 188–192.
- [70] R. Auerbach, Oberflächenspannung und schallgeschwindigkeit, *Experientia* 4 (12) (1948) 473–474.
- [71] J. Hekayati, F. Esmailzadeh, Predictive correlation between surface tension, density, and speed of sound of ionic liquids: auerbach model revisited, *J. Mol. Liq.* 274 (2019) 193–203.
- [72] S. Yu, S. Wang, Z. Tan, C. Liao, Y. Li, Synthesis, characterization and TG-DTA study of diethyl 5-(4-hydroxyethoxyphenylazo) isophthalate, *J. Therm. Anal. Calorim.* 97 (3) (2009) 993–997.
- [73] B. Monteiro, L. Maria, A. Cruz, J.M. Carretas, J. Marçalo, J.P. Leal, Thermal stability and specific heats of coordinating ionic liquids, *Thermochim. Acta* 684 (2020) 178482.
- [74] J.J. Parajó, T. Teijeira, J. Fernández, J. Salgado, M. Villanueva, Thermal stability of some imidazolium [NTf₂] ionic liquids: isothermal and dynamic kinetic study through thermogravimetric procedures, *J. Chem. Thermodyn.* 112 (2017) 105–113.
- [75] M. Shamsipur, S.M. Pourmortazavi, S.S. Hajimirsadeghi, S.M. Atifeh, Effect of functional group on thermal stability of cellulose derivative energetic polymers, *Fuel* 95 (2012) 394–399.
- [76] M.L. Williams, J.S. Dickmann, M.E. McCorkill, J.C. Hassler, E. Kiran, The kinetics of thermal decomposition of 1-Alkyl-3-methylimidazolium chloride ionic liquids under isothermal and non-isothermal conditions, *Thermochim. Acta* (2020) 178509.
- [77] D. Blanco, P. Oulego, D. Ramos, B. Fernández, J. Cuetos, Model-free kinetics applied to evaluate the long-term thermal stability of three [NTf₂] anion-based ionic liquids, *Thermochim. Acta* 656 (2017) 70–84.
- [78] Q. Zhang, Q. Li, D. Liu, X. Zhang, X. Lang, Density, dynamic viscosity, electrical conductivity, electrochemical potential window, and excess properties of ionic liquid N-butyl-pyridinium dicyanamide and binary system with propylene carbonate, *J. Mol. Liq.* 249 (2018) 1097–1106.
- [79] M. Hayyan, F.S. Mjalli, M.A. Hashim, I.M. AlNashef, T.X. Mei, Investigating the electrochemical windows of ionic liquids, *J. Ind. Eng. Chem.* 19 (1) (2013) 106–112.
- [80] M. Faisal, in: *Ionic Liquids As Scavenger*, Green Sustainable Process for Chemical and Environmental Engineering and Science, Elsevier, 2020, pp. 179–198.
- [81] H.N. Gunaratne, P. Nockemann, K. Seddon, Ionic liquids for efficient hydrogen sulfide and thiol scavenging, *Green Chem.* 16 (5) (2014) 2411–2417.
- [82] A.R. Ferreira, M.G. Freire, J.C. Ribeiro, F.M. Lopes, J.G. Crespo, J.A. Coutinho, and COSMO-RS description, *Fuel* 128 (2014) 314–329.
- [83] S. Singh, M. Aznar, N. Deenadayalu, Densities, speeds of sound, and refractive indices for binary mixtures of 1-butyl-3-methylimidazolium methyl sulphate ionic liquid with alcohols at T=(298.15, 303.15, 308.15, and 313.15) K, *J. Chem. Thermodyn.* 57 (2013) 238–247.
- [84] A.B. Pereiro, P. Verdía, E. Tojo, A. Rodríguez, Physical properties of 1-butyl-3-methylimidazolium methyl sulfate as a function of temperature, *J. Chem. Eng. Data* 52 (2) (2007) 377–380.